

Towards an uncertainty analysis for parametric aircraft system noise prediction

Lothar Bertsch¹, Beat Schäffer², and Sébastien Guérin³

¹ DLR, Institute of Aerodynamics and Flow Technology, Bunsenstr. 10, 37073 Göttingen, Germany (corresponding author)

² Empa, Laboratory for Acoustics / Noise Control, Überlandstr. 129, CH-8600 Dübendorf, Switzerland

³ DLR, Institute of Propulsion Technology, Mueller-Breslau-Str. 8, 10623 Berlin, Germany

Corresponding author's e-mail address: lothar.bertsch@dlr.de

ABSTRACT

Parametric noise assessment in the context of low-noise aircraft design and flight procedure optimization has been around for more than 15 years. Continuous improvement of the models and the interconnection to other simulation tools allow today's models to capture the major noise sources and relevant interactions along arbitrary flights. Yet, reliable and comprehensive uncertainty analysis of the overall aircraft noise prediction process has not been available for parametric tools in the past. This paper presents ongoing work to assess the overall uncertainty of DLR's in-house aircraft noise simulation with PANAM, i.e. definition of a general approach to specify uncertainties of the ground noise predictions. This will allow to discuss the temporal and spacial distribution of the uncertainties. Certain areas along a flight path are afflicted with different uncertainties than others. The impact on exposure-response relationships due to the variation in uncertainty will be discussed, i.e. the influence of varying noise source dominance along the simulated flights. Initial results of uncertainties along typical flight procedures and their impact on selected metrics are presented in this contribution.

Nomenclature

acronyms:

DLR	German Aerospace Center
Empa	Swiss Federal Laboratories for Materials Science and Technology
OASPL	Overall Sound Pressure Level: Energetic sum of third-octave band levels
PANAM	Parametric Aircraft Noise Analysis Module
PrADO	Preliminary Aircraft Design and Optimization

input data:

α^*	polar emission angle, [°]
β^*	lateral emission angle, [°]
x_k	k^{th} input parameter, [m, kg, m/s, °K, -]
ϵ_k	k^{th} absolute value uncertainty: input parameter x_k , [m, kg, m/s, °K, -]
R	true relative distance aircraft - observer, [m]
R_{lat}	lateral distance aircraft - observer, [m]
R_{alt}	altitude distance aircraft - observer, [m]

emission:

$L_{em,j}$	component j OASPL, [dB]
$u_{mod,j}$	modelling uncertainty component j , [dB]
$u_{inp,j}$	input data uncertainty component j , [dB]
$u_{e,j}$	total uncertainty component j , [dB]
$u_{em,t}$	total aircraft uncertainty (n components), [dB]

propagation:

ΔL_{geo}	geometric spreading level attenuation, [dB]
u_{geo}	geometric spreading uncertainty, [dB]
u_{atm}	atmospheric absorption uncertainty, [dB]
u_{grd}	uncertainty due to ground reflection modelling, [dB]
u_{prp}	total propagation uncertainty, [dB]

immission:

$L_{A,max,j}$	A-weighted maximum level of component j , [dB]
$L_{A,max}$	total aircraft A-weighted maximum level, [dBA]
$u_{im,t}$	total uncertainty of $L_{A,max}$, [dB]
u_{PAWR}	uncertainty of awakening probability, [%]
P_{AWR}	aircraft noise induced awakening probability, [%]

1 INTRODUCTION

Parametric noise assessment in the context of low-noise aircraft design and flight procedure optimization has been around for more than 15 years. The very first approaches were limited to certain noise sources, used strongly simplified noise source models, and/or were only applicable to simplified and constant flight conditions [1–3]. Continuous improvement of the models and the interconnection to other simulation tools, such as aircraft design codes, allow today's models to capture the major noise sources and relevant interactions along arbitrary simulated flights [4, 5]. Modern simulation processes even enable an automated aircraft design synthesis with integrated noise prediction capabilities [6, 7]. The corresponding prediction tools are also referred to as scientific models [6].

Today's most sophisticated models are physics-based and fully parametrical. They are applied to investigate the interaction of individual noise sources on-board of an aircraft and the effect onto the overall ground noise impact. The main characteristic of such parametrical simulation tools is that a variation of design and operational parameters will directly result in differences in the predicted noise levels. Ultimately, these design and operational parameters can be optimized to result in a minimal ground noise impact. This can only be feasible under careful and simultaneous consideration of all implications to the aircraft design and the corresponding flight performance, i.e. accounting for so-called snowball effects. Only with these modern and sophisticated simulation approaches can the source noise and operational noise of an aircraft be assessed and ultimately be modified simultaneously as it has been postulated by ICAO's Balanced Approach as early as in 2007 [8].

More recent research activities aim at a quantification of result accuracy, i.e. the assessment of uncertainties of the noise level predictions by such parametric simulation tools. Only then, the quality and accuracy of these simulations can be assessed. Reliable and comprehensive evaluation of the overall aircraft noise prediction uncertainties has not been available for the scientific models in the past. In contrast, extensive research towards the uncertainty of predicted aircraft noise levels is documented for conventional or best-practice simulation methods, e.g. FAA's INM or Empa's FLULA2 [9, 11]. Only in the last few months, dedicated activities in the context of scientific simulation methods have been launched at large research institutions such as NASA, ONERA, and DLR. DLR has initiated the *Aircraft Noise Simulation Workgroup* (ANSWr) which among other tasks is dedicated to work on the uncertainty quantification. NASA has recently published first results of their in-house uncertainty analysis for their tool ANOPP 2 [12]. Their analysis focuses on both conventional as well as unconventional aircraft concepts [13]. Furthermore, an uncertainty analysis for noise shielding prediction has been initiated at NASA [14] with shielding being a very promising and effective concept for total aircraft noise reduction [6]. Yet, these recent NASA activities focus on the uncertainty caused by noise source modelling and do not account for the effect of erroneous input data or propagation effects.

This paper will present ongoing DLR activities to assess the overall uncertainty of its in-house simulation process. The presented DLR analysis is still limited to conventional aircraft concepts. This investigation emphasizes the specific impact of erroneous input data and propagation effects in combination with the modelling uncertainties which is not considered in the published NASA study as mentioned before. Ultimately, the goal of the presented analysis is to define a general approach to specify uncertainties for the ground noise levels as predicted by a parametric system noise prediction tool. The NASA study has its focus on the noise certification points, whereas the DLR activity aims at the SPL time-history at arbitrary observer locations. This approach will ultimately allow to discuss the temporal and the spacial distribution of the uncertainties. Certain areas along a flight path can be attributed with different uncertainties than others. The impact of the variation in uncertainty according to the noise source ranking along the simulated flights can be discussed. Initial results of uncertainties along a typical flight procedure are presented and the resulting uncertainty in noise effects are exemplarily estimated for one exposure-response relationship, i.e. aircraft noise induced awakening reactions.

2 NOISE PREDICTION PROCESS

2.1 Tool description

The noise prediction process within conceptual aircraft design as established at DLR and TU Braunschweig is described in various previous publications, e.g. Refs. [3, 6, 7]. The current version of this process can be applied towards a design synthesis of conventional aircraft configurations with an integrated noise analysis. The design synthesis code *Preliminary Aircraft Design and Optimization* (PrADO [15]) of the TU Braunschweig is applied within this study. Noise is predicted with the DLR in-house tool *Parametric Aircraft Noise Analysis*

Module (PANAM [3, 6, 7]) build up from dedicated and parametric noise source models for each of the most important airframe and engine noise components. According to the implemented noise source models, the noise prediction can only be applied to a solution space that is predefined by the inherent characteristics of each model. Only conventional tube-and-wing aircraft with conventional turbofan engines up to by-pass ratios in the order of 15 can readily be analyzed [6]. Yet, additional or updated noise source models can straightforward be integrated.

2.2 Noise source models

The implemented noise source models of PANAM are described in more detail in this section. The selected noise sources models are parametric hence reflect any change in input parameters on their prediction outcome. In other words, the implemented noise source models provide airframe and engine noise radiation characteristics according to the input parameters, i.e. both design and operational input parameters.

These parameters can be modified to study their impact on the predicted noise levels. Possible applications include but are not limited to modifications to vehicle design or flight operation, e.g. flight procedure optimization with respect to community noise annoyance.

The models for airframe noise come from DLR and are described e.g. in Ref. [6]. Overall, five different noise source mechanisms are accounted for, i.e. clean airfoil, leading edge high-lift elements, trailing edge high-lift elements, spoiler, and landing gear. In addition, the impact of flap side-edge noise contribution is modelled with a fully empirical model as described in Ref. [16].

The engine noise is simulated with published models that are commonly accepted and applied. The overall engine is approximated by its two major noise sources, i.e. fan and jet contribution. For fan noise the standard Heidmann [17] model is applied. Empirical coefficients of this model have been adapted to capture more recent engine designs with their reduced fan noise generation. The jet noise contribution is modelled with the classical Stone Jet Noise Model as described in Ref. [18]. Additional modifications to the model are implemented to account for low flight velocities and inverse jet velocities for co-axial jets.

Shielding of engine noise can be evaluated with an external DLR tool, i.e. SHADOW [19]. Dedicated interfaces allow for direct access on the shielding data within a PANAM run. These shielding factors are directly applied to the emission results as predicted by the modified Heidmann model [17]. A dedicated DLR investigation of its noise shielding prediction and the associated uncertainties is scheduled for the near future but not part of the current study. A specific experimental data base is currently built up at DLR in order to enable a dedicated comparison with simulated data [20].

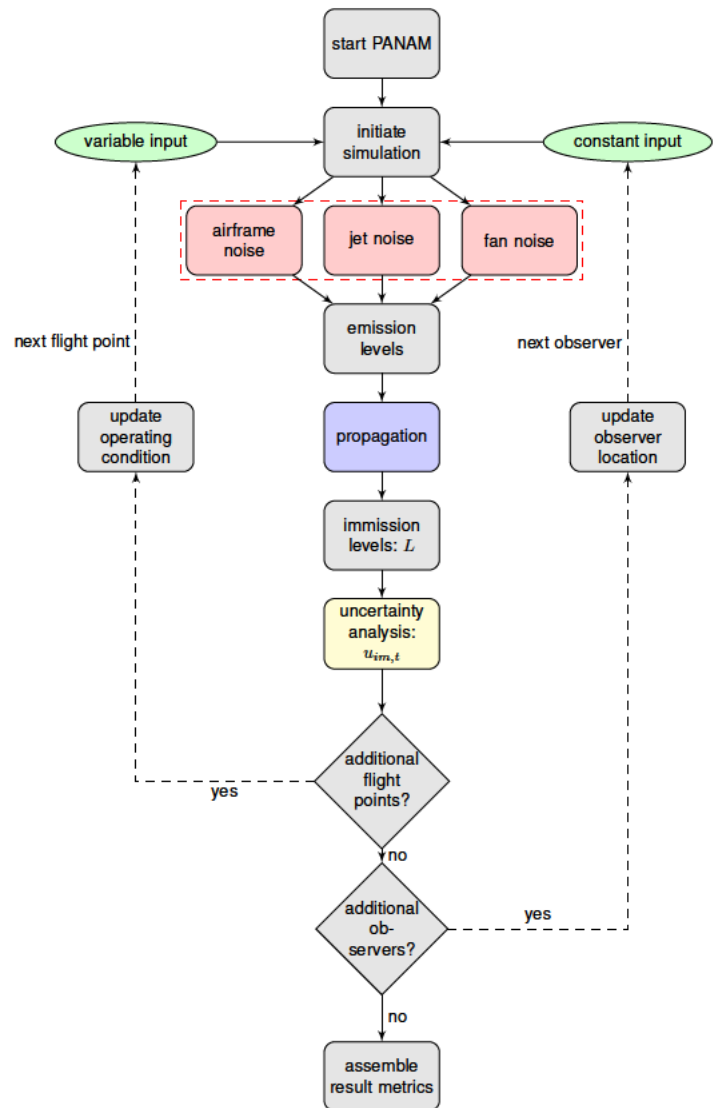


Figure 1: Aircraft noise prediction process (colored boxes: sources of uncertainty).

2.3 Process workflow

The workflow of the prediction process is described in this section and is depicted in Fig. 1. For one observer position at a time, the noise emission from each discrete flight position can be evaluated. According to (1) the aircraft and engine details, (2) the current flight condition / aircraft configuration, and (3) the observer location, the emission levels are predicted. The noise source models provide the farfield SPL frequency spectrum for the relative observer orientation on a reference sphere around the aircraft. To translate the noise characteristics on this reference sphere (emission) to those perceived on the ground (immission), also sound propagation effects have to be accounted for. These effects include geometrical spreading, atmospheric absorption, and ground attenuation. Geometrical spreading for spherical sound sources is applied. The atmospheric absorption is simulated with a simple approach according to the International Organization for Standardization [21]. Ground attenuation in the context of this publication is simulated according to the German standard AzB [22].

The noise signature is assumed to be constant for each single time step referred to as transmission time step. The transmission time step at the observer starts with the first received signal from one flight position. The time step lasts until the emitted sound from the consecutive flight position has reached the observer location. A time-level-history at one certain observer can finally be assembled from the received discrete signals associated with each transmission time step.

The frequency spectrum covers the audible range from 20 to 20 kHz and arbitrary weighting functions for the simulation of human sound perception can be applied to the spectrum, e.g. A-weighting and tone correction. The spectrum can then be transformed into the corresponding overall noise level OASPL. All these steps can be associated with uncertainties as indicated in Fig. 1 by colored boxes. Consequently, the uncertainties have to be analysed for each transmission time step at every observer location.

3 UNCERTAINTY ANALYSIS

In the context of this study, the understanding of the term noise level uncertainty according to Schäffer et al. is underlying [9]: "Calculation uncertainty is defined in analogy to the uncertainty of measurement of Section 2.2.3 in GUM [10] as a parameter, associated with the result of a *model calculation*, that characterises the dispersion of the values that could reasonably be attributed to the *modelling result*."

The analysis is carried out based on sound pressure levels instead of intensities to be consistent with similar activities found in the literature [9, 11, 13, 14, 23]. The standard deviation σ is equivalent to a noise level deviation in ΔdB with respect to the reference level. Working with levels instead of intensities significantly simplifies the problem because now distribution functions can directly be applied to levels in dB and levels are approximately normally distributed. For this initial analysis it is assumed that all uncertainties are normally distributed in their levels, i.e. assuming a standard normal distribution. The standard deviation σ is evaluated, i.e. evaluating the 68% confidence interval.

The setup of the current status of the PANAM uncertainty module is presented in this section and depicted in Fig. 2. The uncertainty module is directly integrated into the overall PANAM workflow (see Fig. 1) and can optionally be executed. A corresponding uncertainty has to be computed along with each predicted noise level along the simulated flight. Only then, the noise source dominance due to aircraft configuration and flight operation can adequately be accounted for.

The uncertainty assessment is performed in a two-step approach, i.e. evaluating the emission uncertainty $u_{em,t}$ and subsequently the immission uncertainty $u_{im,t}$ of the total aircraft noise prediction process. To translate $u_{em,t}$ to the immission uncertainty $u_{im,t}$, the influence of sound propagation u_{prp} has to be accounted for.

3.1 Total aircraft emission: $u_{em,t}$

The total aircraft emission uncertainty $u_{em,t}$ is determined by the individual emission uncertainties of the modeled noise components. PANAM's available noise source models can be categorized into three independent categories: airframe noise models (sum of all individual airframe sources), jet noise model, and fan noise model. These are fully autarkic models, and hence their prediction results and the corresponding uncertainties are not correlated in their statistical behaviour to any of the other two categories [24] and no covariance terms

(see GUM [10]) have to be accounted for. Consequently, an independent emission uncertainty $u_{c,j}$ can be derived for each category j , i.e. airframe, jet, and fan noise uncertainty [24]. If implemented, the effect of fan noise shielding effects can be accounted for in the uncertainty analysis. If structural shielding is applied to the fan noise, the fan noise uncertainty is modified to account for increased uncertainty of the shielding simulation.

Each componential uncertainty u_c is associated with two independent sources of uncertainty. The first uncertainty component is u_{inp} , associated with the uncertainty in input data. u_{inp} is the combined uncertainty with respect to all relevant input parameter uncertainties, i.e. the combination of individual uncertainties $u_{inp,j}$ associated with input parameter x_j and its standard deviation ϵ_j . Secondly, the inherent prediction model uncertainties u_{mod} have to be accounted for. u_{inp} and u_{mod} describe uncertainties for one component or category j in emission levels, i.e. at the source.

Input data

To assess the result uncertainty associated with erroneous input data a sensitivity analysis has been carried out for each component, i.e. for each noise source model. Relevant input parameters for each model under consideration have been varied in a certain range, i.e. $\pm 20\%$, to assess the impact of the parameter change on the predicted noise level. According to the noise source models as implemented in PANAM, predicted levels in dB are linearly dependent on these input parameters.

The impact of an individual parameter variation on the predicted noise level depends on the current operating condition as well as on the relative orientation with respect to the observer, i.e. due to the inherent directivity of the respective noise source. A simple example is used to illustrate the dependency on the operating condition: If the fan operates with maximum rotational speed, the impact of an erroneous rotor-stator-spacing will obviously have a more significant effect on the predicted fan noise compared to a situation with engine idle and other effects predominant. The directivity dependence is less dominant than the effect of the operating condition but still accounted for.

Gradients or sensitivity coefficients $\partial L_{em,j}/\partial x_k$ of the predicted emission levels $L_{em,j}$ of a component j with respect to each independent input parameter x_k can be derived; see Ref. [9]. The dependency of the predicted level $L_{em,j}$ with respect to each x_k has to be evaluated for every operating condition since it is also not constant along a flight¹. Furthermore, the $L_{em,j}$ are predicted for one specific emission angle, i.e. the emission uncertainty analysis is only valid in the direction of one corresponding observer. This sensitivity analysis has to be repeated for every combination of observer location and flight position.

The data variation or uncertainty associated with each input parameter x_k is referred to as ϵ_k . The values

¹ A nearly linear dependency of input parameter x_k and predicted noise level $L_{em,j}$ can be identified under all operating conditions due to the logarithmic scale for levels.

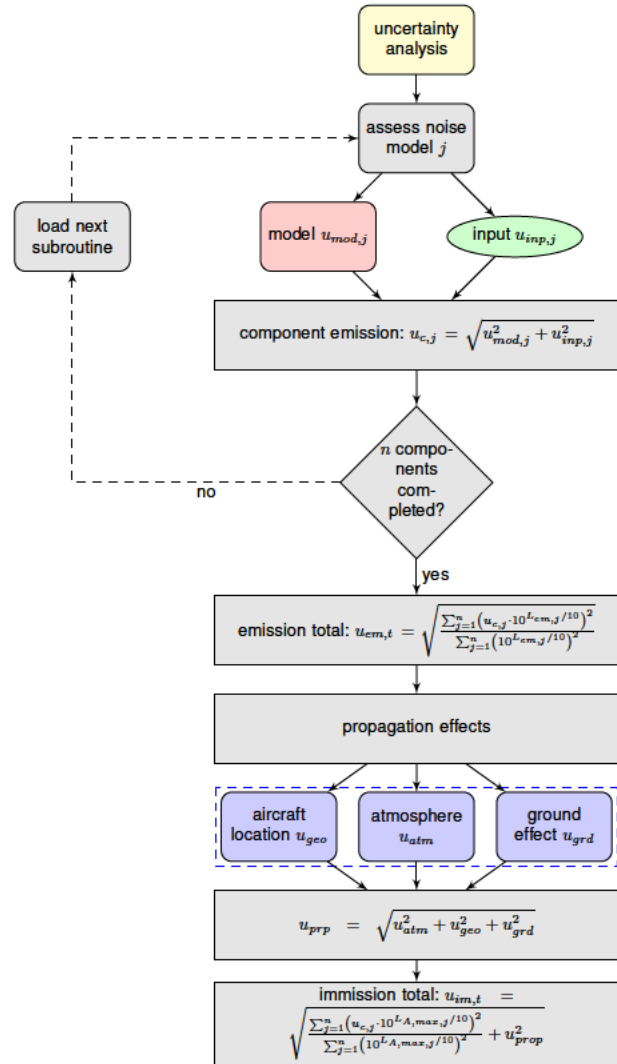


Figure 2: Uncertainty assessment: To be repeated for each flight position and each observer.

of each ϵ_k have to be provided together with the corresponding value for each input parameter x_k or are based on engineering judgement. The effect of one input deviation ϵ_k on the overall predicted level for the underlying operating condition can now be evaluated, i.e. referred to as $u_{inp,k}$.

Gaussian Error Propagation is applied to assess the overall effect caused by all individual $u_{inp,k}$ because the various input parameters are assumed to be independent. All input parameters and their associated uncertainties are assumed to have been independently simulated or measured. For example, the flight altitude as measured by one system with its uncertainty is independent of the flight velocity as measured by another system with its own specific uncertainty. For other parameters it is not that obvious but full independence is assumed for all input parameters and no covariances are evaluated.

The overall input data uncertainty $u_{inp,j}$ per noise source category due to inputs x_k with their ϵ_k can then be derived.

$$u_{inp,j} = \sqrt{\sum_{k=1}^n \left(\frac{\partial L_{em,j}}{\partial x_k} \right)^2 \cdot \epsilon_k^2} \quad (1)$$

The uncertainty due to erroneous input data $u_{inp,j}$ is obviously component specific hence is only valid for the noise source under consideration. To study a new noise sources a separate sensitivity analysis is required in order to generate the specific $u_{inp,j}$ for this very noise source. This sensitivity analysis is only valid for the current operating condition and emission angle.

The input parameters according to Tab. 1 have been preselected for the uncertainty assessment. These parameters represent the most relevant input parameters. Default values for the standard input data uncertainty are based on engineering judgement and experience with aircraft design synthesis codes. These default levels are considered if no more specific information on the ϵ_k values is available. No input data uncertainty for the

category	input parameter	default standard deviation
airframe	TAS (x_1)	$\epsilon_1 = \pm 8 \%$
	t.e. sweep angle (x_2)	$\epsilon_2 = \pm 0.5^\circ$
	i.e. sweep angle (x_3)	$\epsilon_3 = \pm 0.5^\circ$
	wing loading (x_4)	$\epsilon_4 = \pm 10 \%$
fan	N1 (x_1)	$\epsilon_1 = \pm 10 \%$
	RSS (x_2)	$\epsilon_2 = \pm 0.1$
	total mass flow (x_3)	$\epsilon_3 = \pm 10 \%$
	relative tip Mach (x_4)	$\epsilon_4 = \pm 10 \%$
jet	core exhaust velocity (x_1)	$\epsilon_1 = \pm 8 \%$
	bypass exhaust velocity (x_2)	$\epsilon_2 = \pm 5 \%$
	TAS (x_3)	$\epsilon_3 = \pm 8 \%$
	total turbine entry temperature (x_4)	$\epsilon_4 = \pm 10 \%$

Table 1: Selected input parameters with default uncertainties

shielding simulation is considered. To assess the input data uncertainty, the required input data for the shielding simulation, i.e the 3D aircraft geometry, would have to be modified in order to study the results sensitivity. Overall, the precise geometry is expected to have only small influence on the shielding factors as predicted with SHADOW [19].

modelling

Each implemented noise source model comes with an individual and inherent modelling error. The corresponding uncertainty $u_{mod,j}$ for each implemented noise source model can be found in the corresponding literature or tool documentation [6, 17, 25–27]. The airframe and the engine noise models in PANAM have been subject to dedicated validation hence more detailed information on their uncertainties is available. Obviously, the $u_{mod,j}$ are only valid for conventional aircraft types with turbofan engines for which the corresponding noise source models have originally been derived. In contrast to the latest NASA study [13], no model uncertainty $u_{mod,j}$ for application towards unconventional designs is derived or estimated within this study.

Airframe noise prediction as implemented in PANAM is based on DLR's in-house noise source models. These models are described with a standard deviation σ of ± 1 dB [6]. According to the model descriptions, this uncertainty is assumed constant for each airframe source model under consideration.

Engine noise uncertainty is separated into jet noise and fan noise contribution. In general, the predicted levels for conventional turbofan engines up to a bypass ratio in the order of 15 have a standard deviation of ± 4 dB [27]. For a conventional engine design, the fan noise levels are associated with an uncertainty of ± 2 dB according to Ref. [17]. This uncertainty includes the effect of a simulated acoustic lining material in the engine inlet and exhaust ducts. If the fan is subject to noise shielding, an increase in simulation uncertainty has to be expected. Yet, only rough uncertainty estimations based on engineering judgement are available since a dedicated validation is currently still under investigation at DLR as mentioned before. Until more reliable information on the uncertainty of shielding predictions is available, an additional uncertainty of ± 3 dB is selected for the shielded fan noise levels. This selection is based on previous shielding simulation results [19]. The overall modelling uncertainty for a shielded fan therefore is assumed as $\pm\sqrt{2^2 + 3^2}$ dB. This is a valid first assumption since both simulation tools, i.e. the original fan noise model [17] and SHADOW [19], are two fully independent approaches. Jet noise uncertainties are assumed to be somewhat lower than the fan noise uncertainties. A jet noise model uncertainty of ± 1.5 dB is selected for the engine under consideration.

These individual model uncertainties can be assumed valid for other aircraft types as covered by the noise source model definitions, i.e. mid-sized tube-and-wing aircraft with conventional turbofan engines. Tab. 2 summarized the selected modelling standard deviations. Note, that all modelling uncertainties are assumed to be

category	model	literature	standard deviation
airframe	Dobrzynski	Ref. [25]	± 1 dB
fan	modified Heidmann	Ref. [17]	± 2 dB
shielded fan	Lummer	Ref. [19]	± 3.6 dB
jet	Stone	Ref. [18]	± 1.5 dB

Table 2: Selected noise source models with default uncertainties

independent of the operational condition and the emission angle.

Component: $u_{c,j}$

The uncertainty for one individual component is referred to as $u_{c,j}$ and represents the component's emission level uncertainty. The componential $u_{c,j}$ is the sum of modelling and input uncertainty for this very component j .

$$u_{c,j} = \sqrt{u_{mod,j}^2 + u_{inp,j}^2} \quad (2)$$

For each implemented noise source category j an independent $u_{c,j}$ can be computed for one underlying operating condition. Along a flight procedure, u_c is not constant but will change due to varying input data, i.e. u_{inp} will change whereas the modelling uncertainty u_{mod} is constant by definition. The input data uncertainties are dependent on both the emission angle and the operating condition.

Total emission: $u_{em,t}$

The total aircraft emission uncertainty $u_{em,t}$ is assembled from all the individual component emission uncertainties. Consideration and summation of each $u_{c,j}$ and the predicted noise emission $L_{em,j}$ will result in a value for $u_{em,t}$. This total aircraft emission uncertainty is obviously highly dependent on the actual operating condition, i.e. the noise source ranking, and therefore is not constant along a simulated flight. Obviously, a dominating noise source will have more impact on the predicted $L_{em,j}$ and $u_{em,t}$ than a less dominant source. Along any approach and departure flight, the noise source ranking is significantly varying hence the uncertainty level can be expected to change accordingly. Consequently, an energetic weighting is applied to translate the different componential $u_{c,j}$ to one overall $u_{em,t}$. The methodology is described by various researchers in the literature [9–11, 24]. The weighting with the individual uncertainty $u_{c,j}$ is applied to the predicted noise levels $L_{em,t}$ of this very component.

$$u_{em,t} = \sqrt{\frac{\sum_{j=1}^n (u_{c,j} \cdot 10^{L_{em,j}/10})^2}{\sum_{j=1}^n (10^{L_{em,j}/10})^2}} \quad (3)$$

3.2 Sound propagation: u_{prp}

The total aircraft noise emission uncertainty $u_{em,t}$ is translated to the immission uncertainty $u_{im,t}$ by accounting the influence of sound propagation effects, i.e. effects due to a simulated propagation through the atmosphere. These effects are geometrical spreading, atmospheric attenuation, and ground attenuation. The corresponding uncertainties are referred to as u_{geo} , u_{atm} , and u_{grd} , respectively.

The overall uncertainty due to these three (assumed) uncorrelated effects is the total propagation uncertainty u_{prp} and is derived by Gaussian Error Propagation:

$$u_{prp} = \sqrt{u_{geo}^2 + u_{atm}^2 + u_{grd}^2} \quad (4)$$

Geometrical spreading: u_{geo}

To assess the noise level uncertainty due to an erroneous aircraft location the approach by Schäffer et al. is selected [9]. The locations are defined relative to the observer location under consideration. The effect of an erroneous relative location can directly be correlated with the change in geometrical spreading ΔL_{geo} for spherical sound propagation.

$$\frac{\partial(\Delta L_{geo})}{\partial R} = \frac{-20}{R \cdot \ln(10)} = \frac{-8.69}{R} \quad (5)$$

The erroneous aircraft location is approximated according to Schäffer et al. [9] by selecting a standard deviation for the lateral location R_{lat} and the altitude R_{alt} of the aircraft with respect to the observer. The selection of the lateral standard deviation is $\epsilon_{lat} = 133 \text{ m}$ and the altitude standard deviation is $\epsilon_{alt} = 27 \text{ m}$. The aircraft location standard deviation is referred to as ϵ_{loc} .

$$\epsilon_{loc} = \frac{\sqrt{R_{lat}^2 \cdot \epsilon_{lat}^2 + R_{alt}^2 \cdot \epsilon_{alt}^2}}{R} \quad (6)$$

Based on ϵ_{loc} the effect on the geometrical spreading uncertainty can be derived.

$$u_{geo} = \sqrt{\left(\frac{-8.69}{R}\right)^2 \cdot \epsilon_{loc}^2} = 8.69 \cdot \frac{\epsilon_{loc}}{R} \quad (7)$$

Atmospheric attenuation: u_{atm}

Atmospheric attenuation for one individual flight is complex and can be in the order of 10s of dB [28]. The atmospheric attenuation is dependent on the frequency, distance, and ambient conditions, hence a different u_{atm} for each noise source would be required. In the context of this work the atmospheric attenuation uncertainty is simplified and approximated with the method by Schäffer [9]. The method reflects the fact of raising uncertainty due to atmospheric propagation with increasing distance to the observer.

$$u_{atm} = 1.0 + 0.0003 \cdot R \quad (8)$$

This simplification is used for all noise sources at the moment independent of their frequency content.

Ground attenuation: u_{grd}

The uncertainty due to ground attenuation effects with the underlying algorithm [22] is approximated as $u_{grd} = \pm 1 \text{ dB}$ at the moment. This is in agreement with the estimate by Schäffer [9].

3.3 Total aircraft immission: $u_{im,t}$

In the context of this study, the emission analysis is fully independent and not correlated with the assessment of the propagation effects. Hence, the emission results can simply be translated into the immission situation. In order to account for the noise source ranking at the observer, the corresponding A-weighted immission levels are processed here.

$$u_{im,t} = \sqrt{\frac{\sum_{j=1}^n (u_{c,j} \cdot 10^{L_{A,max,j}/10})^2}{\sum_{j=1}^n (10^{L_{A,max,j}/10})^2} + u_{prop}^2} \quad (9)$$

The total aircraft noise uncertainty $u_{im,t}$ is inherent for the simulation of one specific aircraft along a specific flight for one specific receiver point. It can now be assessed for arbitrary observer locations along a simulated flight. The uncertainties $u_{im,t}$ are consecutively evaluated for each discrete time step of the simulation at each one observer location. Assembling the discrete time steps at the specified observer location will yield both

the predicted immission levels and their associated uncertainties $u_{im,t}$ as a function of time. At this point it is assumed that each individual level along a time-history is independent of each other hence no co-variances are evaluated. This is valid for the assessment of maximum levels but will have to be modified if integrated levels are evaluated, e.g. the Sound Exposure Level.

The time-history will directly yield the predicted A-weighted maximum noise level and the corresponding level of uncertainty at that instant. Hence, isocontour plots of the total aircraft noise uncertainty can be generated. The uncertainty correlated with the maximum noise level on the ground is stored for each observer and the spacial distribution can be analyzed.

4 INITIAL RESULTS

The presented methodology with the default setting² is now applied to assess prediction uncertainties for a reference vehicle³ simulated along a typical approach flight procedure. The selected noise metric is the maximum A-weighted Sound Pressure Level $L_{A,max}$ at predefined observer locations on the ground.

An exemplary $L_{A,max}$ footprint is depicted in Fig. 3 along with the underlying flight trajectory of the aircraft. Levels for the overall aircraft and for the components fan, jet, and airframe are depicted. Along the flight, the individual noise contributions vary according to the operational setting, i.e. configuration, flight velocity, and thrust setting. Fig. 4 shows exemplary the emitted noise levels and the corresponding uncertainties for two operating conditions, i.e. with engine or airframe dominating. Obviously, each flight position along the simulated flight has a different emission situation. Therefore, each flight position is assessed individually to finally propagate to the ground and assemble the immitted level and uncertainty.

Fig. 5 shows the spacial distribution of the associated immission uncertainties. As expected, the componential uncertainty of the dominating noise source defines the overall uncertainty. Areas of higher and lower uncertainty can be identified and associated with the underlying noise source ranking. If "bad" input data is selected, the input data uncertainty become significantly large.

The maximum levels $L_{A,max}$ can now further processed based on an exposure-response relationship, i.e. the propability P_{AWR} of additional awakenings due to a nocturnal single flyover event as defined by Basner [29]. To translate the predicted outdoor levels to indoor levels (partly opened window), a difference between inside and outside $L_{A,max}$ of 15 dB is assumed according to Ref. [29].

$$P_{AWR} = 1.894 \cdot 10^{-3} \cdot L_{A,max}^2 + 4.008 \cdot 10^{-2} \cdot L_{A,max} - 3.3243 \quad (10)$$

At this point, any inherent uncertainty of the P_{AWR} function is not considered. Then, the uncertainties associated with the predicted P_{AWR} can directly be attributed to the $L_{A,max}$ uncertainties. A sensitivity coefficient can be derived to finally yield the uncertainty of the exposure-response relationship P_{AWR} as a function of the $L_{A,max}$ uncertainty.

$$u_{P_{AWR}} = \sqrt{\left(\frac{\partial P_{AWR}}{\partial L_{A,max}}\right)^2 \cdot u_{im,t}^2} \quad (11)$$

As expected, the isocontour areas are similar to the $L_{A,max}$ contours, see Fig. 6. The uncertainty of the exposure-response relationship is depicted in Fig. 7. The predicted awakening propability is in the order of 0 to 10% with an uncertainty up to 1.5%. The underlying $L_{A,max}$ are in the order 40 to 90 dB. The associated uncertainties are in the range of 2 dB close to the aircraft with dominating airframe noise up to 5 dB and more for observers far from the flight ground track.

5 CONCLUSION

A new approach towards the assessment of uncertainties for conventional aircraft has been presented. The overall goal is to establish a quality assessment for the system noise prediction at DLR. The presented assessment is limited to the parametric noise prediction of a single event! No conclusions should be drawn with respect to large scenarios with multiple flights along different routes over very long time frames. The presented analysis is understood as an essential and indispensable step towards any future application of parametric tools including more unconventional vehicle concepts or advanced flight procedure design. A good understanding of the inherent simulation capabilities is essential if one is depending on simulation results only. Only

² Input data uncertainties as defined in Tab. 1.

³ Conventional mid-range transport aircraft: 3300 km design range, 125 PAX, and a cruise Mach of 0.76.

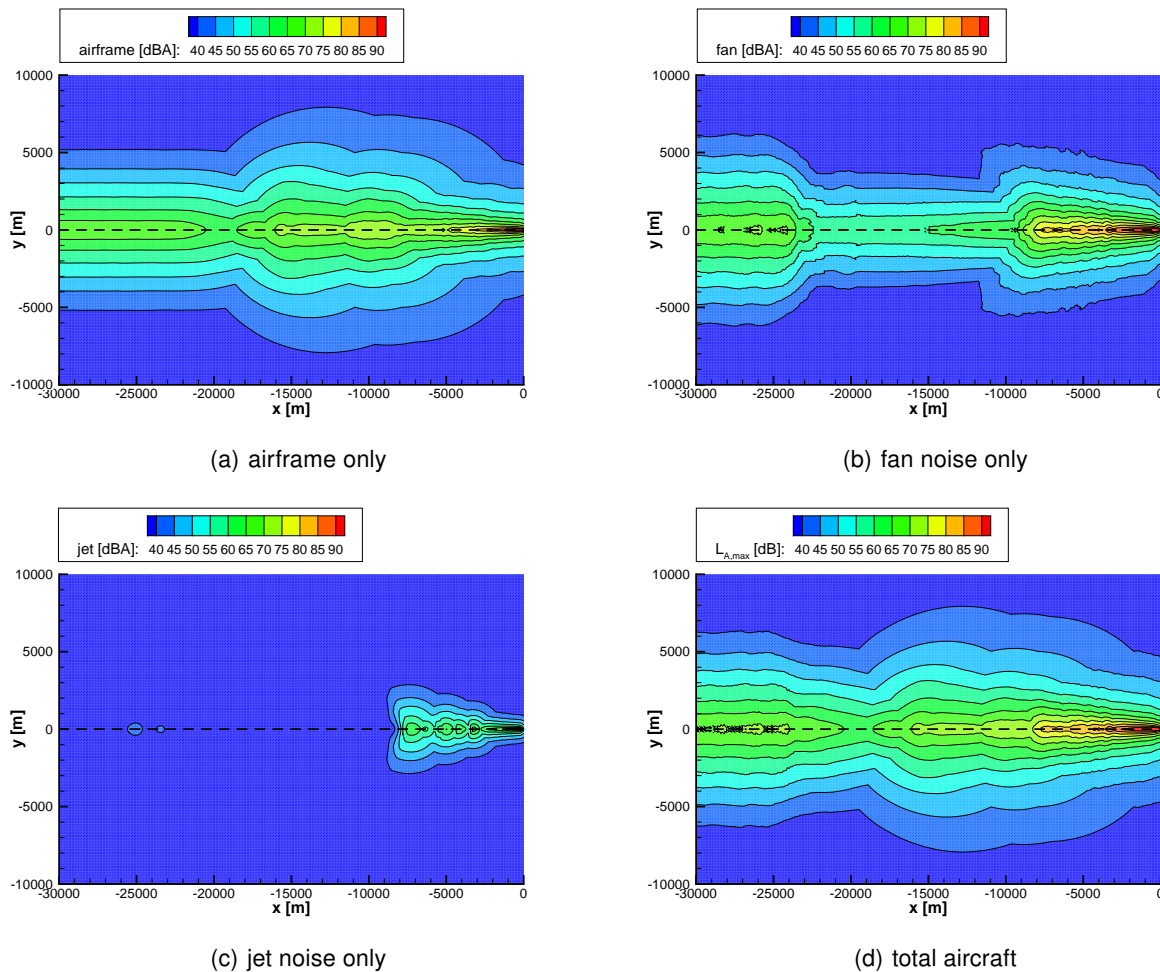


Figure 3: Isocontour areas of total and componential $L_{A,max}$ along approach (flight ground track: dashed line; touch-down: at $x = 0$ m)

if the uncertainties of the predicted levels are known, a reliable assessment seems feasible. Therefore, an uncertainty module has been integrated into DLR's PANAM software to predict the uncertainty associated with each predicted emission and immission level. In contrast to previous work on uncertainty analysis of parametric tools the input and propagation uncertainties have been included in the analysis. It can be demonstrated that both effects can even exceed the uncertainties of the noise source models when simulating conventional vehicles. Moreover, if the input data quality is furthermore reduced, significant increase in uncertainty can be demonstrated.

Future work

Any comparison with other simulation tools or experimental data requires the knowledge of the underlying uncertainties within the process. Therefore, the simulated levels with uncertainties will ultimately be compared to existing experimental data from DLR flyover noise campaigns, e.g. of an A319 [25], to judge the validity of the predictions. This kind of assessment will help to better understand deviations between simulation results and experimental data. With a system level uncertainty information, observed deviations might directly be associated with the modelling uncertainty of an individual noise source or the input data uncertainty. Furthermore, more significant deviations as experienced for observer locations in large distance to the aircraft might be explained by the uncertainties of the simple propagation simulation. If no such correlation can be identified, the result deviation must be caused by other influences that are not adequately accounted for, e.g. parasitic airframe noise sources that are not modelled. It is expected to gain a much better understanding of the entire simulation process after such a dedicated comparison with experimental data.

Ultimately, the simplifications as selected for this initial uncertainty assessment will be replaced by more sophisticated approaches. In the long term, adaption to the predefined default uncertainties of the noise source

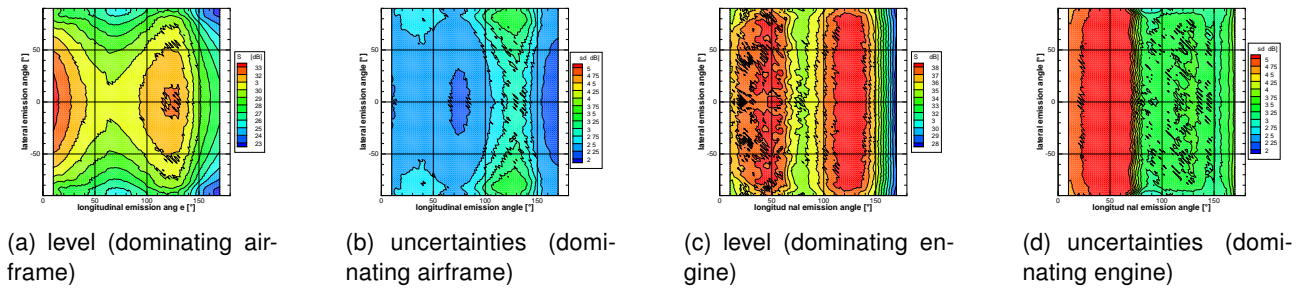


Figure 4: Predicted levels and uncertainties for different operating conditions (emission on 1 m sphere)

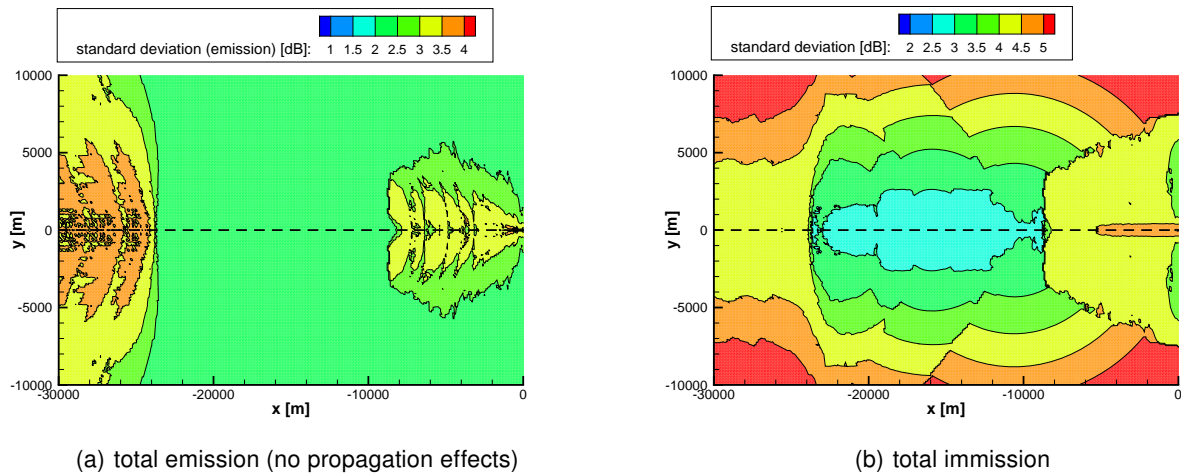


Figure 5: Isocontour areas of predicted uncertainties along approach

models have to be adapted to account for various other aircraft designs. The latest findings with respect to uncertainties in the simulation of noise shielding will be included. Furthermore, new noise source models with their inherent uncertainties will be implemented into PANAM to enable an uncertainty assessment for novel aircraft configurations.

ACKNOWLEDGMENTS

This work has partially be funded by the DLR internal project *Future Enhanced Aircraft Configurations* and the DLR *Projektförderung zur Internationalen Zusammenarbeit*. The analyses presented here are associated with the *Aircraft Noise Simulation Workgroup (ANSWr)*, a joint NASA, ONERA, and DLR research activity.

References

- [1] N. E. Antoine, I. M. Kroo: *Framework for Aircraft Conceptual Design and Environmental Performance Studies*, AIAA Journal, Vol. 43, No. 10 (2005), pp. 2100-2109
- [2] E. D. Olson, D. N. Mavris: *Aircraft Conceptual Design and Risk Analysis Using Physics-Based Noise Prediction*, AIAA-2006-2619, 12th AIAA/CEAS Aeroacoustics Conference, 2006
- [3] L. Bertsch, W. Dobrzynski, S. Guérin: *Tool Development for Low-Noise Aircraft Design*, 14th AIAA Aeroacoustics Conference, DOI: 10.2514/6.2008-2995, 2008
- [4] M. Brunet, T. Chaboud, N. Huynh et al.: *Environmental Impact Evaluation of Air Transport Systems Through Physical Modelling and Simulation*, AIAA-2009-6936, 9th AIAA Aviation Techn., Integration, and Operations Conference, 2009
- [5] Y. Guo, C. L. Burley, and R. H. Thomas: *On Noise Assessment for Blended Wing Body Aircraft*, 52nd Aerospace Sciences Meeting, 2014, DOI: 10.2514/6.2014-0365, 2014
- [6] L. Bertsch: *Noise Prediction within Conceptual Aircraft Design*, DLR research report, ISSN 1434-854, ISRN DLR-FB-2013-20, 2013

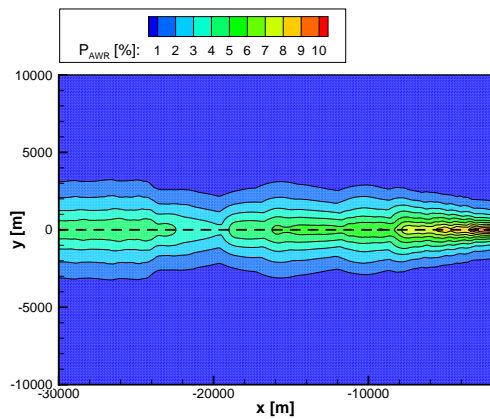


Figure 6: P_{AWR} isocontour areas

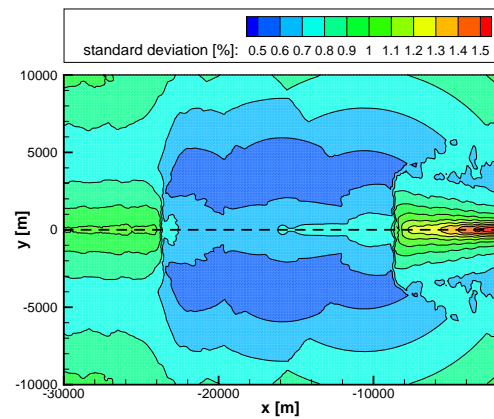


Figure 7: Uncertainties of P_{AWR}

- [7] L. Bertsch, W. Heinze, M. Lummer: *Application of an Aircraft Design-To-Noise Simulation Process*, 14th AIAA Aviation Technology, Integration, and Operations Conference, DOI: 10.2514/6.2014-2169, 2014
- [8] International Civil Aviation Organization (ICAO), Air Transport Bureau (ATB): *Concept of a balanced approach principle to aircraft noise management*, appendix C of Assembly Resolution A35-5, 2007
- [9] B. Schäffer, S. Pluess, G. Thomann: *Estimating the model-specific uncertainty of aircraft noise calculations*, Applied Acoustics, special issue: air transport noise, Volume 84, pages 58-72, ISSN: 0003-682X, 2014
- [10] *Uncertainty of measurement: Guide to the expression of uncertainty in measurement*, Guide 98-3, Geneva, Switzerland: International Organisation for Standardization (ISO) and International Electrotechnical Commission (IEC), 2008
- [11] G. Thomann: *Uncertainties of measured and calculated aircraft noise and consequences in relation to noise limits*, PhD Thesis ETH Zuerich, No. 17433, 2007
- [12] V. Lopes, C. L. Burley: *Design of the Next Generation Aircraft Noise Prediction Program: ANOPP2*, 17th AIAA/CEAS Aeroacoustics Conference (32nd AIAA Aeroacoustics Conference), Portland, Oregon, 5-8 June, 2011
- [13] R. H. Thomas, C. L. Burley, and Y. Guo: *Progress of Aircraft System Noise Assessment with Uncertainty Quantification for the Environmentally Responsible Aviation Project*, 22nd AIAA/CEAS Aeroacoustics, 10.2514/6.2016-3040, 2016
- [14] C. L. Burley, R. H. Thomas, and Y. Guo: *Quantification of Acoustic Scattering Prediction Uncertainty for Aircraft System Noise Assessment*, 22nd AIAA/CEAS Aeroacoustics Conference, DOI: 10.2514/6.2016-3041, 2016
- [15] W. Heinze: *Ein Beitrag zur quantitativen Analyse der technischen und wirtschaftlichen Auslegungsgrenzen verschiedener Flugzeugkonzepte für den Transport groSSer Nutzlasten*, Zentrum für Luft- und Raumfahrt, Rept. 94-01, Technische Univ. Braunschweig, Brunswick, Germany, 1994
- [16] K.-S. Rossignol: *Development of an empirical prediction model for flap side-edge noise*, AIAA-2010-3836, 16th AIAA/CEAS Aeroacoustics Conference, 7 - 9 June 2010, Stockholm, Sweden
- [17] Heidmann: *Interim prediction method for fan and compressor source noise*, NASA Tech. Report, TMX-71763, 1979
- [18] J. R. Stone, D. E. Groesbeck, C. L. Zola: *Conventional profile coaxial jet noise*, AIAA Journal, 21(1) (1983), pp. 336-342
- [19] M. Lummer: *Maggi-Rubinowicz Diffraction Correction for Ray-Tracing Calculations of Engine Noise Shielding*, 14th AIAA/CEAS Aeroacoustics Conference 2008, paper AIAA-2008-3050
- [20] K. S. Rossignol, J. Delfs: *Analysis of the Noise Shielding Characteristics of a NACA0012 2D Wing*, AIAA 2016-2795, 22nd AIAA/CEAS Aeroacoustics Conference, DOI: 10.2514/6.2016-2795, 2016
- [21] International Organization for Standardization, ISO: *standard ISO 9613-1:1993*, 1993
- [22] Bundesministerium der Justiz: *Erste Verordnung zur Durchführung des Gesetzes zum Schutz gegen Fluglärm* (Verordnung über die Datenerfassung und das Berechnungsverfahren für die Festsetzung von Lärmschutzbereichen-1.FlugLSV), Bundesgesetzblatt BGBl I, 27th December 2008
- [23] M. Dahl: *A Process for Assessing NASA's Capability in Aircraft Noise Prediction Technology*, 14th AIAA/CEAS Aeroacoustics Conference, DOI: 10.2514/6.2008-2813, 2008
- [24] W. Probst, U. Donner: *Die Unsicherheit des Beurteilungspegels bei der Immissionsprognose*, Zeitschrift für Lärmbekämpfung, Volume 49, pages 86-90, 2002
- [25] M. Pott-Pollenske et al.: *Airframe Noise Characteristics from Flyover Measurements and Predictions*, AIAA-2006-2567, 12th AIAA Aeroacoustics Conference, 2006
- [26] Bridges, Kharavan, Hunter: *Assessment of Current Jet Noise Prediction Capabilities*, AIAA-2008-2933, 14th AIAA Aeroacoustics Conference, 2008
- [27] Envia, et. al: *An Assessment of Current Fan Noise Prediction Capability*, AIAA-2008-2991, 14th AIAA Aeroacoustics Conference, 2008
- [28] M. J. T. Smith: *Aircraft Noise*, Cambridge Aerospace Series, Cambridge University Press, ISBN 0-521-61699-9, 2004
- [29] M. Basner, B. Griefahn, M. Berg: *Aircraft noise effects on sleep: mechanisms, mitigation and research needs*, Noise & Health Journal, Vol. 12 (47), pages 95-109, 2010